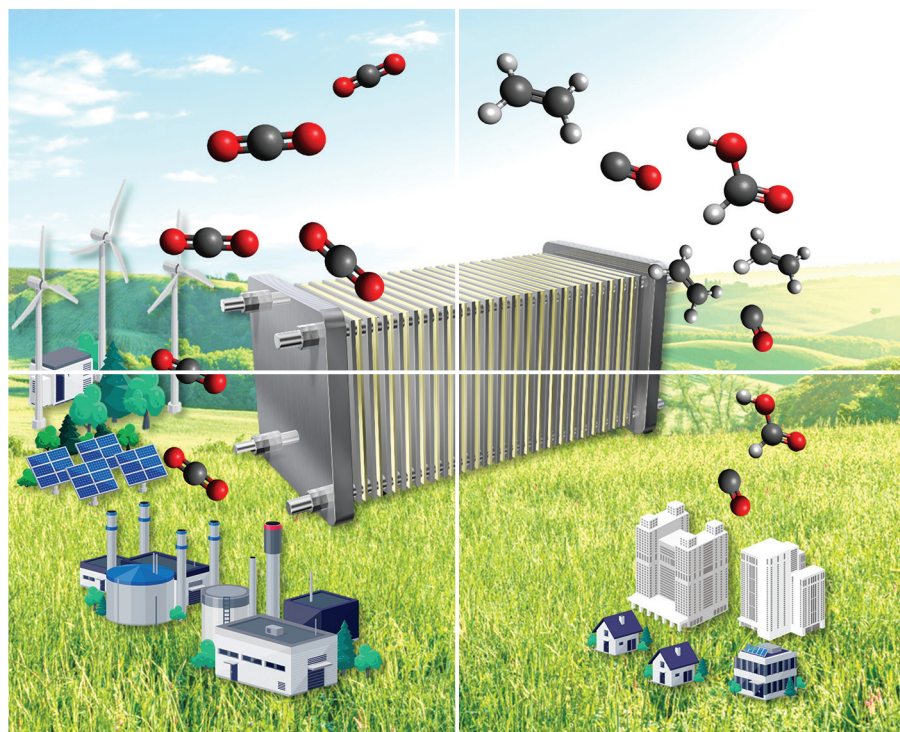


Volume 10 | Number 24 | 21 December 2023

**10**  
YEARS  
ANNIVERSARY



# INORGANIC CHEMISTRY

## FRONTIERS



CHINESE  
CHEMICAL  
SOCIETY



ROYAL SOCIETY  
OF CHEMISTRY

[rsc.li/frontiers-inorganic](https://rsc.li/frontiers-inorganic)

## REVIEW

View Article Online  
View Journal | View IssueCite this: *Inorg. Chem. Front.*, 2023,  
10, 7095Recent advances in electrocatalytic reduction of ambient CO<sub>2</sub> toward high-value feedstockNaohiro Fujinuma \*<sup>a</sup> and Samuel E. Lofland \*<sup>b</sup>

The effects of climate change have arisen due to greenhouse gases emitted into the atmosphere, and the finite supply of fossil fuels will eventually be unable to support the needs of the petrochemical industry. Solutions to these two complex problems will have to be multipronged, but the industrial implementation of the electrocatalytic reduction of CO<sub>2</sub> can help with both issues. Importantly, the demand for multi-carbon feedstock offers immediate financial incentives, accelerating the search for solutions to the climate problem. However, the technology for the electrocatalytic reduction of CO<sub>2</sub> is still in the process of being commercialised, and the use of ambient CO<sub>2</sub> is a prerequisite for widescale adoption. Here we discuss the progress in this area and the remaining barriers to realizing its potential.

Received 3rd August 2023,  
Accepted 10th October 2023

DOI: 10.1039/d3qi01522j

rsc.li/frontiers-inorganic

## 1. Introduction

Nature has a rich history of converting CO<sub>2</sub> into valuable resources driven by the abundant renewable energy from the sun. Carbon monoxide dehydrogenase/acetyl-CoA synthase, the main enzymatic complex in thousands of types of bacteria, has been remarkably effective in microorganisms for more than 3.5 billion years, fixing CO<sub>2</sub> as a carbon resource.<sup>1</sup> In contrast, human beings have only enjoyed highly energy-intensive modern life since the industrial revolution, powered by oxidising energetically compressed fossil fuels. This process results in the reverse carbon flow from underground to the atmosphere. This anthropogenic oxidative carbon consumption accounts for the rise of atmospheric CO<sub>2</sub> levels, as illustrated by the Keeling Curve.<sup>2</sup> Consequently, the United Nations has declared “a code red for humanity”, warning that the concentration of atmospheric greenhouse gases poses a threat to lives, economies, health and food security.

A desired pathway is to aggressively implement renewable energies, which would consequently lead to a dramatic shift in the material production scheme from the fossil-fuel dependent supply chain to one that relies on more sustainable resources. The CO<sub>2</sub> reduction reaction (CO<sub>2</sub>RR) has the potential to play a pivotal role in accelerating such a material evolution due to its attractive natural features: it occurs under atmospheric reaction conditions, does not require any side reactants such as hydrogen, is compatible with renewable energy resources, and offers a wide range of potential products.

A literature search shows that the CO<sub>2</sub>RR study dates back as far as the 1950s as a way to produce chemicals.<sup>3,4</sup> In the 1980s and 90s, comprehensive research was conducted on a variety of metal or molecular catalysts and electrolytes to discuss the selectivity of CO<sub>2</sub>RR.<sup>5–7</sup> As predicted by Hori,<sup>7</sup> there has been a significant resurgence in the use of CO<sub>2</sub>RR within the research community in recent years, resulting in an increasing number of publications equivalent to Moore’s law (Fig. 1). Despite its long history and the renewed focus on developing efficient and selective electrocatalysts, CO<sub>2</sub>RR has not been adopted by conventional chemical industries as a replacement for fossil fuels. This is in contrast to lithium-ion battery technology, which was discovered later but has been widely commercialised with an even steeper rise in the publication rate.

Why has nature successfully implemented ambient CO<sub>2</sub> reduction, while the same achievement has thus far eluded

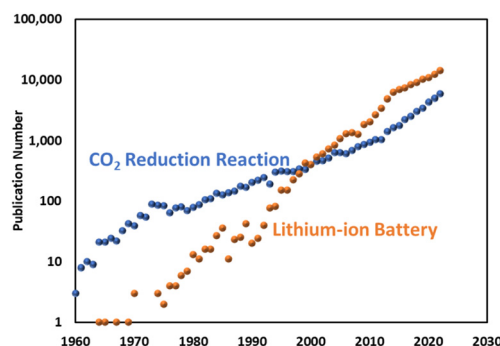


Fig. 1 Annual publications for an electrocatalytic CO<sub>2</sub> reduction reaction and lithium-ion battery research.

<sup>a</sup>Sekisui Chemical Co., Ltd, 2-4-4 Nishitemma, Kita-ku, Osaka 530-8565, Japan.  
E-mail: fujinuma@rowan.edu

<sup>b</sup>Department of Physics and Astronomy, Rowan University, 201 Mullica Hill Rd.,  
Glassboro, NJ 08028, USA. E-mail: lofland@rowan.edu

human ingenuity? With this question in mind, we will discuss several important aspects of CO<sub>2</sub>RR. However, given the breadth of research in this field, this review does not seek to be exhaustive; rather, it aims to provide insight into the economic viability and future of CO<sub>2</sub>RR. First, we introduce the potential products of CO<sub>2</sub>RR, followed by a techno-economic analysis to shed light on the current barriers towards the successful commercialization of CO<sub>2</sub>RR. Finally, we will review a few studies dealing with the less-discussed but significant properties for successful CO<sub>2</sub>RR implementation.

## 2. Basic principles and catalyst science for CO<sub>2</sub>RR

One of the attractive but complicating features of CO<sub>2</sub>RR is that it has a variety of possible products along with competing hydrogen evolution reaction (HER), all of which have similar standard redox potentials *vs.* reversible hydrogen electrode derived from the Gibbs energy and physicochemical constant.<sup>8</sup> Due to the close thermodynamic characteristics of CO<sub>2</sub>RR, the selectivity of the expected CO<sub>2</sub>RR is dependent on both the modulation of electrochemical activation energy toward a specific route and the availability of the corresponding reactants. An electrochemical catalyst is needed to lower the activation energy of a specific target by stabilising an intermediate for the reaction. CO<sub>2</sub>RR is an inner-sphere reaction involving multiple electron- and proton-transfer processes. In contrast to an outer-sphere reaction, in which the electron transfer occurs through tunnelling across a monolayer of solvents, the heterogeneous inner-sphere reaction is based on the interaction of a reactant, a product, or an intermediate with the catalyst surface. These interactions enable a critical intermediate species more likely to be structurally changed in subsequent steps.

As a principle, the rate of the multi-step reaction is determined by the slowest step, *i.e.*, the rate-determining step (RDS). It has been proposed that two-electron transfer reactions of CO<sub>2</sub>RR into CO or HCOOH may possess different types of RDS.<sup>9–11</sup>

As for CO<sub>2</sub>RR into CO and HCOOH (Fig. 2), steps 1 and 5 represent the CO<sub>2</sub> adsorption process which triggers the CO<sub>2</sub>RR pathway. A recent study indicates that this process can be dependent on the applied potential because of the inter-

action between the dipoles of the participating reaction intermediates with the interfacial field.<sup>10,11</sup> Both field-dependent density functional theory and pH-dependent activity measurements concluded that the ideal catalyst should possess large adsorbate dipoles on CO<sub>2</sub>\*.<sup>10</sup> Steps 2 and 6 are concerted proton–electron transfer steps, and the configuration of CO<sub>2</sub>\* seems to determine the selectivity with transition metal surfaces.<sup>12</sup> One computational study<sup>13</sup> suggests that the C-atom bonding structure leads to the CO production pathway while an O-atom mediated bond is more likely to induce formate/formic acid production. Experimental studies such as *in situ* surface Raman scattering confirm that such a configurational change determines the selectivity of the CO<sub>2</sub>RR product.<sup>14,15</sup> Steps 1' and 5' are proton-decoupled electron-transfer steps whose kinetics are independent of the number of local protons in the vicinity of the catalytic site, followed by the protonation to form COOH or OCOH [steps 2' and 6']. The final step of CO<sub>2</sub>RR is the desorption of a product from the catalytic site [steps 4 and 8]. Since the electrochemical activation energy expectedly correlates with the adsorption energy between the intermediate species of the rate determining step and the catalytic sites, the free energy of the adsorption of the intermediate is usually discussed to elucidate the catalyst selectivity.

## 3. Techno-economic analysis of CO<sub>2</sub>RR in the context of performance matrices

Since CO<sub>2</sub>RR is an alternative way to produce existing fossil fuel-derived catalysts, the electro-synthesized product needs to compete economically with the widely-established market products. In this context, a techno-economic analysis (TEA) should be considered and included in the discussion of studies which investigate the application of CO<sub>2</sub>RR. One of the simplest ways to approximate the economic validity of CO<sub>2</sub>RR products is to plot the relationship between the minimum energy requirement for the targeted product and the corresponding market price. Here the minimum energy consumption per unit mass  $E_{\min}$  is defined by

$$E_{\min} = n(E_{\text{red}}^{\circ} - E_{\text{min}}^{\circ})F/MW \quad (1)$$

where  $n$  is the electron number for a specific reaction,  $E_{\text{red}}^{\circ}$  is the standard redox potential for CO<sub>2</sub>RR,  $E_{\text{ox}}^{\circ}$  is the standard redox potential for the counter reaction,  $F$  is the faradaic constant, and  $MW$  is the molar mass of the product.

The thermodynamic cell potential serves as an indicator of the minimum energy requirement for a given product and thus, given the energy costs, provides a means to estimate the economic viability of a product. Fig. 3 shows the possible CO<sub>2</sub>RR products plotted as a function of  $E_{\min}$  and market price as of 2023. One notices that CO and formic acid are well positioned in this proximity of economic analysis due to its two-electron transfer characteristics. Some oxygenates such as acetic acid and acetaldehyde also possess a relatively high



Fig. 2 Reaction schemes for the CO<sub>2</sub> reduction reaction into CO or HCOO.

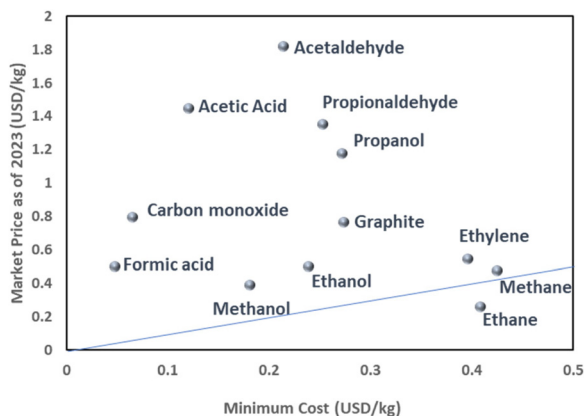


**Fig. 3** Possible electrocatalytic CO<sub>2</sub> reduction reaction products plotted as a function of minimum energy consumption per unit mass and market price as of 2023. The line represents the break-even point assuming no additional financial incentives.

market value compared to the required minimum cost. Alcohol derivatives and graphite materials are in the middle group because of the moderate minimum costs and current economic value. As the carbon number in the alcohol increases, the minimum cost and current market price increase concomitantly, indicating that the market price reflects the energy required for the chemical supply. The graph also highlights the challenges of synthesizing hydrocarbon products such as ethylene, methane, and ethane. The discrepancy between the low market price and the high-cost characteristics of these derivatives is attributed to the fundamental differences between the processes in the existing petrochemical infrastructure and in a future CO<sub>2</sub>-based electrochemical supply. Specifically, hydrocarbons can be extracted from fossil fuels without additional energy to convert chemical structures since nature has already converted CO<sub>2</sub> into hydrocarbons over a long period of time. By contrast, CO<sub>2</sub>RR needs additional energy to convert CO<sub>2</sub> into hydrocarbons, which inevitably adds costs relative to fossil-fuel-derived hydrocarbons. Since hydrocarbons are a fundamental commodity for the chemical industry, subsidies are likely needed for the timely implementation of CO<sub>2</sub>RR to support the hydrocarbon chemical chain.

Note that recent electrocatalyst and photocatalyst studies have demonstrated the combination of CO<sub>2</sub>RR and an unconventional anode reaction to either reduce the cell voltage<sup>16</sup> or directly synthesize more complex chemicals,<sup>17,18</sup> which may pave the way toward an efficient CO<sub>2</sub>RR production system.

While the minimum cost approximation is helpful to identify the economic potential of CO<sub>2</sub>RR targets, the actual TEA should be more in-depth. There are three basic process steps for CO<sub>2</sub>RR: CO<sub>2</sub> purification, CO<sub>2</sub> conversion, and product purification (Fig. 4). The TEA of the overall chemical process reminds us of what we need to rapidly scale up the CO<sub>2</sub>RR and, in turn, provides key insights for essential future studies.

The cost associated with CO<sub>2</sub> purification depends on the CO<sub>2</sub> ratio of the initial gas mixture and a capture method. CO<sub>2</sub> captured from concentrated CO<sub>2</sub> sources, such as power and



**Fig. 4** Basic processes for a scaled-up electrocatalytic CO<sub>2</sub> reduction reaction: CO<sub>2</sub> purification, CO<sub>2</sub> conversion, and product purification.

chemical plants or from amine technology, has the lowest price of \$50–70 t<sup>-1</sup> with a US Department of Energy target of \$40 t<sup>-1</sup>.<sup>19</sup> On the contrary, capturing CO<sub>2</sub> from the air is more expensive than from flue gas because of its low concentration: one study estimated that the cost for CO<sub>2</sub> capture from the air could potentially reach ≈\$100–200 t<sup>-1</sup> in the future.<sup>20</sup> The cost of CO<sub>2</sub> purification in a typical carbon conversion unit provides an opportunity to pursue new technology to simplify or eliminate CO<sub>2</sub> purification. If effluent gas is converted in the CO<sub>2</sub> conversion unit on site in places such as fired power plants or incineration plants, the cost for the CO<sub>2</sub> purification step decreases. In addition, the degree of required CO<sub>2</sub> purification depends on how sensitive the CO<sub>2</sub> conversion is to the impurities in the gas stream entering the CO<sub>2</sub> conversion. For instance, NO<sub>x</sub> and SO<sub>x</sub> are usually present in exhaust gas and the effects of these oxide impurities on the selectivity and durability of the CO<sub>2</sub>RR catalyst are still largely unexplored.

The CO<sub>2</sub>RR product purification process includes gas and/or liquid separation, depending on the physicochemical properties of the production. Gas separation is usually required because of the presence of unconverted CO<sub>2</sub> and unintended side products such as H<sub>2</sub> in the product effluent. Liquid product separation is often required to extract products in the liquid catholyte. Pressure swing adsorption (PSA) and membrane technologies are currently used in other industrial processes with similar gas compositions.<sup>21</sup> It appears that PSA is generally preferred because of its relatively low operating costs and high efficiency with an estimated cost of around \$10 t<sup>-1</sup> based on CO<sub>2</sub>RR TEA<sup>22</sup> and the Sherwood plot for the separation of dilute streams.<sup>23</sup> Liquid product separation can be executed through distillation, extraction, precipitation, and pervaporation.<sup>21</sup> Among these, distillation is widely used but it is expected to have a much higher operational cost than gas separation with PSA.

The operational cost of the CO<sub>2</sub>RR product depends on the purity of the target and chemical composition in the product stream from the electrochemical conversion unit. Thus, both the selectivity and conversion ratio of CO<sub>2</sub>RR are imperative to determine the energy required for the purification process. In addition, the additives for the electrochemical reaction, such as electrolyte salts and co-catalysts, should be considered in the cost analysis for the product separation process.



The CO<sub>2</sub> conversion unit operates predominantly with electricity as input energy and CO<sub>2</sub> as feedstock. Therefore, the energy efficiency in converting CO<sub>2</sub> into target chemicals, defined as the ratio of thermodynamic energy to input energy, affects the operational cost of CO<sub>2</sub>RR. Energy efficiency is a function of the sum of the overpotential of cathodic and anodic reactions along with other voltage drops in an electrolyser and FE for the specific product. CO<sub>2</sub>RR into hydrocarbon such as ethylene usually requires prominent overpotential to kinetically drive the reaction, which may push up the operational costs. As for the CO<sub>2</sub> feedstock, the conversion ratio of CO<sub>2</sub> as a system affects the operational cost as the unconverted CO<sub>2</sub> is either wasted or requires more energy to be recycled. The CO<sub>2</sub>RR cell is preferably designed to minimize CO<sub>2</sub> loss. For instance, when an alkaline electrolyte is used on the cathode side, CO<sub>2</sub> loss likely occurs as a dissolved carbonate, preventing the efficient utilization of CO<sub>2</sub>. One strategy is to utilize a fully carbonated system with an anion exchange membrane, which leads to the consumption of CO<sub>2</sub> at the cathode and the re-emission of CO<sub>2</sub> with oxygen at a locally acidic anode. However, an additional separation step is required to recover CO<sub>2</sub> from the anode vapours.

As for the capital cost, the partial current density, the observed current for the relevant reaction per geometric area, is important to determine the total electrode size of the electrolyser for the CO<sub>2</sub>RR. Given that the number of electrons to be transferred varies depending on the CO<sub>2</sub>RR reaction, a more practical manner to evaluate the productivity of CO<sub>2</sub>RR may be to convert current density into the production rate of the targeted product per geometric area.

The durability of the CO<sub>2</sub> converting unit or electrochemical cell is also an important factor in affecting the frequency of cell replacement and the operational cost. TEA studies often use a lifecycle of 5–30 years.<sup>22,24,25</sup> However, conventional CO<sub>2</sub>RR studies usually report durability results for times of 10–100 h, and there is a gap between the current testing period and the prolonged durability test required before building the actual plant. Moreover, an accelerated testing protocol needs to be designed to speed up the durability development, which is also currently not well addressed. The definition of the reduction in performance at which the CO<sub>2</sub>RR cell should be replaced will remain an open question until key stability/durability relationships are experimentally established.

One should note that the CO<sub>2</sub>RR process can reduce or increase CO<sub>2</sub> emissions depending on the energy required for the total production process and the carbon intensity of the electricity and utilization. The carbon intensity of renewable energy is significantly lower than that of fossil fuel-derived electricity, suggesting the combination of the CO<sub>2</sub>RR process and such renewable energy can be a more carbon-neutral scheme. In this case, integrating the CO<sub>2</sub>RR process into the off-grid renewable energy should be discussed since the plant system requires additional electric equipment, such as energy storage systems and converters. A hydrogen production electrolyser plant powered by renewable energy can be a good model for estimating the cost impact of electricity management in a CO<sub>2</sub>RR plant.

The source of CO<sub>2</sub> and electricity significantly affects the cost of the CO<sub>2</sub>RR process and the benefit of CO<sub>2</sub> emission reduction. The CO<sub>2</sub>RR process prefers more concentrated CO<sub>2</sub> sources in the fluent gas. However, we should envision the long-term viability of CO<sub>2</sub> emitters since the social system will require a change toward more carbon-neutral structures. The electricity price changes significantly depending on the region, the electricity resources, and geopolitical environments. Since the CO<sub>2</sub>RR plant is an electricity-demanding process, one needs to choose the place to develop the plant carefully. Usually, TEA applies an electricity cost of 0.02–0.03 USD per kW per h,<sup>22,24,25</sup> which still limits the actual short-term option to scale up the CO<sub>2</sub>RR process, which can reflect the cost simulation of the TEA.

After providing an overview of TEA, we propose emphasizing the following domains in the plant flow (CO<sub>2</sub> concentration, conversion, and the production purification step) for scaling up CO<sub>2</sub>RR deployment (Fig. 5): (1) the effect of chemical composition of the feed gas, (2) the industrially relevant productivity and durability of CO<sub>2</sub>RR, and (3) maximizing the CO<sub>2</sub> conversion ratio and optimizing selectivity to minimize the need for purification processes.

## 4. Noteworthy CO<sub>2</sub>RR research toward economically valuable feedstock

### 4.1. Effect of the chemical composition of feed gas

Most CO<sub>2</sub>RR research has been carried out with concentrated CO<sub>2</sub>, which helps increase the reaction rate and selectivity of CO<sub>2</sub>RR due to the high availability of CO<sub>2</sub> at catalytic sites and avoids undesirable side reactions stemming from impurities. As mentioned in section 3, the CO<sub>2</sub> concentration process, while relatively mature, introduces additional energy consumption and costs to implement CO<sub>2</sub>RR, which may induce unfavourable CO<sub>2</sub> emissions. Therefore, it is desirable that the CO<sub>2</sub>RR is compatible with direct effluents from CO<sub>2</sub> sources. The CO<sub>2</sub> concentration of fired power plants is around 15% (v/v), depending on the type of fossil fuels and combustion

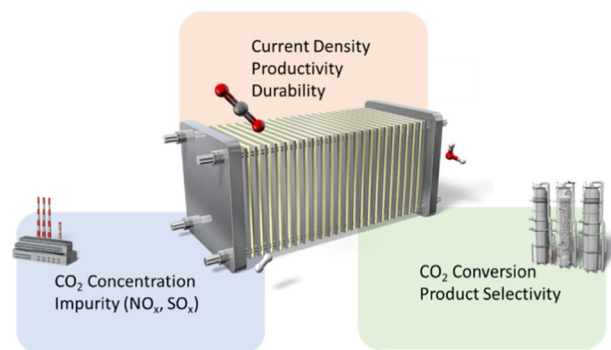


Fig. 5 The highlighted research domain in the process flow of the electrocatalytic CO<sub>2</sub> reduction reaction.

system. Also, industry exhaust streams often contain other gaseous species such as  $N_2$ ,  $O_2$ ,  $H_2O$ ,  $NO_x$ ,  $SO_x$ , and volatile organic compounds. The oxidized components of flue gas, such as  $SO_x$  and  $NO_x$ , may influence  $CO_2RR$  catalysts, although their concentrations are low (typically in the order of hundreds of ppm). Therefore, deviating from pure  $CO_2$  gas could impact the  $CO_2RR$  catalytic activity and durability.

The decrease in  $CO_2$  partial pressure is expected to decrease the reaction rate of  $CO_2RR$  when  $CO_2$  diffusion is a rate-limiting step. This is the case for electrolysis under the practical conditions of operating close to the maximum partial current density regardless of the structure of the electrolyser cell. Additionally, the decreased  $CO_2$  partial pressure creates a reaction environment preferable to the competing HER since the number of protons for the reaction is independent of the gas component. Moreover, the adverse effect of limited  $CO_2$  in the incoming gas may become more severe as the size of the electrolyser increases because the consumption of  $CO_2$  in the gas or electrolyte occurs along with the plane of the electrode, and the gas/liquid stream close to the outlet of the flow cell has the lowest amount of  $CO_2$ . Therefore, the influence of  $CO_2$  partial pressure is a vital factor in determining the compatibility of  $CO_2RR$  with the exhaust gas.

There have been some studies on the effect of  $CO_2$  partial pressure and presenting engineering-based strategies to tackle limitations. Among the pioneering studies in the 1990s,<sup>26,27</sup> Komatsu observed that the current density and FE for  $CO_2RR$  decreased as  $CO_2$  concentration decreased from 100 to 14% with the copper composite electrode for the gas-phase  $CO_2RR$ .<sup>28</sup> Consistent with that work, Kenis *et al.*<sup>29</sup> reported that the partial current density noticeably decreased with the decrease in the  $CO_2$  concentration with Ag nanoparticle catalysts on the gas diffusion electrode in the  $CO_2/N_2$  mixture feed in 1 M KCl electrolyte media. The authors also observed the decrease in the FE for  $CO_2RR$  to CO by using phosphate buffer as the electrolyte to distinguish between the effect of  $CO_2$  partial pressure and pH in the electrolyte. The pH dependency study showed that the FE for  $CO_2RR$  to CO decreased more severely with the decrease in pH, suggesting that the number of local protons initiates the HER, diminishing  $CO_2RR$  more easily as either the  $CO_2$  concentration in the feed or the pH in the electrolyte decreased.

A straightforward way to address the diluted  $CO_2$  concentration is to elevate the pressure of the electrolyser system, which increases  $CO_2$  availability at the catalyst. Xu *et al.*<sup>30</sup> demonstrated that the pressurization of the feed gas at 15 bar successfully maintained a 91% FE for  $CO_2RR$  to CO with 15% (v/v)  $CO_2$ , which is similar to or higher than that of the performance with pure  $CO_2$  at 1 bar, depending on the applied potential. While pressurization requires some additional energy input, they calculated that the energy required to pressurize to 10 bar represents only ~3% of the energy required to perform efficient  $CO_2RR$  to  $C_2$  products. These results indicate that pressurization helps enable the direct conversion of streams with  $CO_2$  concentrations characteristic of major flue gas sources at industrially relevant current densities.

$O_2$  is the highest concentration reactive impurity in flue gas and is challenging to remove. The oxygen reduction reaction has a more favourable thermodynamic potential and kinetics compared to  $CO_2RR$ , which significantly impedes the target selectivity. As an initial study, Morikawa *et al.*<sup>31</sup> confirmed that the inclusion of  $O_2$  significantly reduces the FE for  $CO_2RR$  to formate with a porous ruthenium complex polymer catalyst on a photocathode from 93% (at 0%  $O_2$ ) to 6% (at 7%  $O_2$ ) due to the selective  $O_2$  reduction competing with  $CO_2$  reduction. They demonstrated that the combination of the catalyst with carbon papers mitigated the drop of FE to 75% at 7%  $O_2$ , which is attributed to the affinity of the carbon materials to gaseous  $CO_2$  in aqueous solution, resulting in the relatively concentrated  $CO_2$  in the vicinity of the catalytic sites. However, the measurement of local  $CO_2$  should be carried out for further discussion.

Exploiting the difference in solubility between  $CO_2$  and  $O_2$  in the electrolyte media is one way of mitigating the parasitic effect of  $O_2$ . Sinton *et al.*<sup>30</sup> exploited an ionomer and  $TiO_2$  coating to create a hydrophilic environment around the Cu catalysts so that  $CO_2$  can predominantly dissolve and reach the catalytic sites over  $O_2$ . They observed a FE towards  $C_2$  products of 68% and energy efficiency of 26% over 10 h of stable operation (at 10 bar), a performance competitive with some of the best results previously reported on reactors using pure  $CO_2$ .

Another methodology to circumvent the oxygen reduction reaction is to implement an additional layer to selectively transport or adsorb  $CO_2$  over  $O_2$ . Wang *et al.*<sup>32</sup> demonstrated that a polymer of intrinsic microporosity serves a role in selectively permitting  $CO_2$  to permeate while preventing  $O_2$  from reaching the catalytic sites. They coated the gas separation polymer on the opposite side of the carbon paper of the cobalt phthalocyanine catalyst and observed FE for CO of 75.9% in a gas with 5%  $O_2$  in contrast to the catalyst without the gas separation layer performing no observable FE with the same  $O_2$  concentration. Subsequently,<sup>33</sup> the authors applied aniline molecules to enhance the ability of the permeable ionic membrane (PIM) to separate  $CO_2$  from  $O_2$  using chemical interactions between the acidic  $CO_2$  and the basic amino group of aniline. In an electrolytic flow cell with a cobalt phthalocyanine/carbon nanotube catalyst, they observed a FE for CO of 71% in the presence of 10%  $O_2$  in  $CO_2$  using the PIM/aniline membrane, therefore outperforming the pure PIM with a FE for CO of 63% under the same conditions. While these studies highlight the effectiveness of structurally or chemically engineering the microstructure, further research regarding the physicochemical properties of  $CO_2$  and O combined with kinetic modelling will lead to clearer design principles for selective  $CO_2$  supply in a microenvironment.

$NO_x$  is among the major contaminants present in industrial  $CO_2$  point sources with a typical concentration of 10–500 ppm depending on the regional regulation and combustion system.<sup>34</sup>  $NO_x$  usually consists of 90–95% NO and 5–10%  $NO_2$ ,  $N_2O$  being a common by-product formed in the  $NO_x$  removal process. All of these  $NO_x$  gases can compete with  $CO_2$  for electrons through the corresponding reduction reaction, which

has a more favourable standard redox potential than CO<sub>2</sub>RR. Therefore, the kinetics of the NO<sub>x</sub> reduction reaction, along with the concentration of NO<sub>x</sub>, could be crucial factors to be investigated. Moreover, NO<sub>2</sub> can also react with water to produce various acidic products, including nitric and nitrous acids.

Komatsu *et al.*<sup>28</sup> found no effect of 200 ppm NO on the catalytic activity of gas-phase CO<sub>2</sub>RR with a copper-deposited electrode. The author argued that the amount of NO was about two times higher than that of the exhaust gas from a typical coal-fired power plant. Jiao *et al.*<sup>35</sup> demonstrated that the presence of much higher amounts of NO, NO<sub>2</sub>, and N<sub>2</sub>O (8300 ppm) in the CO<sub>2</sub> feed leads to a considerable FE loss in CO<sub>2</sub>RR with Cu, Ag, and Sn catalyst-loaded gas diffusion electrodes. Notably, they observed the recovery of the FE for CO<sub>2</sub>RR after switching the feed gas without NO<sub>x</sub>, suggesting that NO<sub>x</sub> is involved in the electroreduction process but does not affect the structure of the catalysts in these conditions. In addition, they evaluated the effect of 830 ppm and 83 ppm NO, showing less severe (less than 5%) and negligible losses in FE, respectively, highlighting that CO<sub>2</sub>RR can be compatible with typical concentrations of NO<sub>x</sub> in flue gases. Note that the parasitic effect of NO<sub>x</sub> is dependent on the nature of the catalyst and an electrochemical setup. Oh *et al.*<sup>36</sup> reported a decrease in FE for HCOO<sup>-</sup> from 69.4% to 37.7% using SnS<sub>x</sub> as the catalyst in the presence of 90 ppm NO. Sridhar *et al.*<sup>37</sup> observed a loss in FE for ethylene of 22.9% after exposing the copper catalyst to 1% NO<sub>2</sub> and a change in the surface colour of the copper catalyst, showing that excessive NO<sub>2</sub> may contribute to the oxidation of the catalysts.

SO<sub>x</sub> is another possible chemical component in the gas feed. Typical power plants emit exhaust containing 10–300 ppm SO<sub>2</sub>. Komatsu *et al.*<sup>28</sup> found that 170 ppm SO<sub>2</sub> in the feed noticeably changed the distribution of the products with a copper catalyst. Jiao *et al.* observed a general decrease in the FE for total CO<sub>2</sub> reduction after copper, silver, and tin catalysts were exposed to a gas stream of 1% SO<sub>2</sub> in CO<sub>2</sub>, which is attributed to the preferential reduction of SO<sub>2</sub>. Silver and tin catalysts showed less change in the product distribution and the recovery of FE for each product was attained after stopping the feed of SO<sub>2</sub>. However, the catalyst characterization shows the sulfurization and desulfurization reaction of Ag and Sn after the SO<sub>2</sub> and pure CO<sub>2</sub> feed, respectively, inferring that these materials are relatively durable against the sulfur-derived structural change. On the contrary, the exposure of SO<sub>2</sub> causes the product distribution with Cu catalysts toward formate, which is irreversible even after switching back to a pure CO<sub>2</sub> stream. The authors attributed the change to residual Cu<sub>2</sub>S formed on the surface.

One finds that there is a sizeable difference between the amount of impurities used for the CO<sub>2</sub>RR studies mentioned above and the actual content found in the exhaust from specific CO<sub>2</sub> sources. This is because the emitters have often already modified the fraction of impurities to prevent air pollution. Therefore, in more practical scenarios, the tested chemical composition for CO<sub>2</sub>RR needs to match the actual

composition for a true feasibility study. Investigations into the effects of impurities on the durability of the CO<sub>2</sub>RR catalyst should also be conducted. Since the existing CO<sub>2</sub> purification process, such as the amine adsorption method, already works to reduce the impurities, the total design of combining the CO<sub>2</sub> purification and conversion relies on the efficiency and durability of the CO<sub>2</sub>RR process.

Current CO<sub>2</sub>RR demands a high CO<sub>2</sub> partial pressure compared to nature, which converts 440 ppm CO<sub>2</sub> with highly diluted solar energy. While direct air capture is in the pilot phase of plant testing, the general cost for concentrating CO<sub>2</sub> from a level of a few hundred ppm to nearly 100% is unacceptably high due to the intensive energy required for the process. One option would be combining the CO<sub>2</sub> concentrator and a converter compatible with significantly diluted CO<sub>2</sub> sources, but resolving the issues surrounding gas impurities needs to be addressed first.

#### 4.2. Industrially relevant productivity and durability of CO<sub>2</sub>RR

While the FE and energy efficiency for a specific product affect the operational cost of electrolysis, the current density or productivity per geometric surface area of the electrode is essential in determining the capital cost since as the productivity increases, the size of the electrolyser decreases. The current density is typically one of the matrices used to evaluate CO<sub>2</sub>RR research. A practical measure is the productivity of the specific product per specific time and the electrode geometric area.

Fig. 6a shows the reported partial current density and expected production rate per day for various products.<sup>33–126</sup> HCOOH/HOO<sup>-</sup> has the highest value of production rate per partial current density due to its 2-electron transfer characteristics and relatively high molecular weight, followed by CO production. CO<sub>2</sub> to ethanol or ethylene has a lower production rate per partial current density because these products require 12 electrons to be transferred to the reactant but have a similar molecular weight.

Significant efforts to improve the partial current density have been made in the last few years, mainly focusing on the catalyst design to increase the catalytic site density and electrochemical cell engineering to achieve gas-phase reactions to cir-

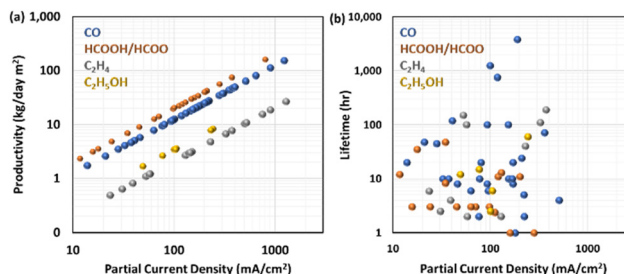


**Fig. 6** (a) The expected production rate per day as a function of the partial current density for each CO<sub>2</sub>RR product with the experimental data according to the literature survey. (b) Reported lifetime of CO<sub>2</sub>RR as a function of the partial current density for each CO<sub>2</sub>RR product with the experimental data according to the literature survey.

cumvent the limitations of CO<sub>2</sub> solubility in the electrolyte. The flow or membrane electrode assembly (MEA) cell configuration with a gas diffusion electrode especially has played a central role in creating a three-phase boundary environment where CO<sub>2</sub> can encounter the catalytic sites and ions as a counterpart for the CO<sub>2</sub>RR reaction. In addition, recent studies<sup>127</sup> have introduced micropores or a hydrophobic environment in the catalytic layer to accumulate CO<sub>2</sub> near the catalytic sites.

Sun *et al.*<sup>128</sup> demonstrated a hierarchical nanoporous catalyst by retaining the micropores of a metal–organic framework precursor to enhance CO<sub>2</sub> concentration in the gas-diffusion electrode, achieving 645 mA cm<sup>-2</sup> CO partial current density at -0.53 V vs. RHE with 86% FE for CO under ambient conditions, which is equivalent to a production rate of 80 kg d<sup>-1</sup> m<sup>-2</sup>. Chen *et al.*<sup>78</sup> developed a cell with 450 mA cm<sup>-2</sup> partial current density with 90% FE for formate with a SnO<sub>2</sub> electrocatalyst. This corresponds to an impressive production rate of 88 kg d<sup>-1</sup> m<sup>-2</sup>. Liao *et al.*<sup>129</sup> implemented a Ni–N<sub>5</sub>–C single atom catalyst in a flow cell configuration, achieving industrial-scale performance for CO<sub>2</sub>RR to CO a FE of 97% at a current density reaching a maximum of 1.23 A cm<sup>-2</sup> with an FE of 99.6%, the highest production rate of CO<sub>2</sub>RR to CO of 154 kg d<sup>-1</sup> m<sup>-2</sup> to date. The authors attributed the high performance to the Ni–N<sub>5</sub> catalytic site, which is superior in activating CO<sub>2</sub> molecules and reducing the energy barriers for the intermediate binding energy for boosting the kinetic activation process and catalytic activity. Endrödi *et al.* employed a PiperION membrane for electrocatalytic CO<sub>2</sub> reduction to CO in a tailored zero-gap electrolyser.<sup>130</sup> This membrane possesses high carbonate-ion conductivity, leading to a high CO current density (over 1 A cm<sup>-2</sup>) with commercial Ag nanoparticles while maintaining a high FE for CO (up to 90%).

In contrast to the recent rapid advancement of the productivity of CO<sub>2</sub>RR, industrially relevant durability has not been achieved yet. Many durability tests (Fig. 6b), including the aforementioned industrially viable production rates, are in the range of 10–100 h. There are only a few studies on CO<sub>2</sub>RR to CO that report durability test results over 1000 h long. Notably, one case<sup>44</sup> involves a commercially available anion-exchange membrane (Sustainion) incorporated in MEAs, which illustrated at least 3800 hours of activity at 190 mA cm<sup>-2</sup> with FE for CO<sub>2</sub>RR to CO of 95% with a silver nanoparticle cathode and an IrO<sub>x</sub> anode. The authors implemented two strategies to keep the membrane hydrated: (1) humidifying CO<sub>2</sub> and (2) circulating deionized water or diluted KHCO<sub>3</sub> solution in the anode.

In general, more thorough durability testing is required. So far, only *ex situ* and after-use characterization has been carried out for the CO<sub>2</sub>RR electrolyser. There is an urgent need to develop conditions for accelerated testing and then correlating the results between accelerated aging and actual performance.

### 4.3. Minimizing the purification process

Here we suggest distinguishing between two performance metrics regarding the CO<sub>2</sub>RR conversion. One is the CO<sub>2</sub> con-

version efficiency (CE<sub>CO<sub>2</sub></sub>) defined as the ratio of the amount of CO<sub>2</sub> converted into a target to the amount of CO<sub>2</sub> fed into the system. Another important but less discussed factor is product selectivity, defined as the fractional amount of the target product within the total stream. The former is relevant to the cost of CO<sub>2</sub> consumption and recovery if necessary, and there are some recent studies focused on CE<sub>CO<sub>2</sub></sub>. The latter is important to determine how much energy is needed to purify the product in the following chemical process. The electrochemical cell can be divided into the cathode and anode compartments, and a path for the product stream is not always the same as the CO<sub>2</sub> flow pathway since the CO<sub>2</sub> can cross the membrane; CE<sub>CO<sub>2</sub></sub> is often independent of the product selectivity.

Most CO<sub>2</sub>RR studies have been carried out in neutral and alkaline electrolytes to impede HER, in which the high current density often creates a strongly alkaline microenvironment at the cathodic interface. This consumes some CO<sub>2</sub> in the feed through sequential chemical reactions of CO<sub>2</sub> driven by the pH gradient in the cell.<sup>66,132,133</sup> Specifically, an unfavourable reaction between CO<sub>2</sub> and OH<sup>-</sup> produces carbonate or bicarbonate, which subsequently crosses the anion exchange membrane to the anode, reacts with H<sup>+</sup> from the oxygen evolution reaction, and is converted to CO<sub>2</sub> in the anode tail gas, giving rise to a low theoretical single pass conversion rate of 50%. Moreover, bicarbonates precipitate with alkaline metals at the cathode once their local solubility hits the limit, which closes microchannels for CO<sub>2</sub> and ion for the CO<sub>2</sub>RR and causes a degradation mode.<sup>134</sup> It is expected that regenerating lost CO<sub>2</sub> demands additional energy and operating costs.

One adopted strategy for overcoming the CO<sub>2</sub> carbonation problem is to provide CO<sub>2</sub> regeneration space between the catalytic layer and an ion exchange membrane while maintaining the anionic micro-environment in the vicinity of the catalytic site. This methodology has been implemented by including additives in the catalyst layer or inserting an additional buffer layer.<sup>124,135,136</sup>

O'Brien *et al.*<sup>135</sup> developed a permeable CO<sub>2</sub> regeneration layer, which provides an alkaline environment at the CO<sub>2</sub>RR catalyst surface and enables local CO<sub>2</sub> regeneration concomitantly. They coated the copper cathode layer with the functional groups of the anion exchange polymer (Aemion AP1-CNN5-00-X) to create a positive space charge, enabling the transport of anions and impeding the cations. The polymer coating on the cathode allows for CO<sub>2</sub> transport to the catalyst *via* diffusion through the water-filled hydrated ionic domains in the polymer matrix. With the careful tuning of the thickness of the regeneration layer of ~10 μm to minimize impedance to CO<sub>2</sub> and water, they attained 85% CE<sub>CO<sub>2</sub></sub> with a cation exchange membrane (Nafion 117) and deionized water. The authors proposed that the positively charged functional groups in the polymer structure act as a positive charge as an alternative to alkali metal cations, which can stabilize CO<sub>2</sub>RR intermediates to promote C–C coupling on copper catalysts.

Li *et al.*<sup>136</sup> demonstrated that an acid-fed MEA for CO<sub>2</sub> electroreduction to CO with an H<sup>+</sup> to Cs<sup>+</sup> satisfies both the FE and



conversion efficiency of CO<sub>2</sub>. Essentially, an anion-exchange ionomer with quaternary ammonium side chains was incorporated into the Ag catalyst layer to shield the Ag surface from a high proton flux and provide diffusion pathways for dissolved CO<sub>2</sub> and water. After optimizing ion concentrations and operation parameters, they observed a single-pass conversion efficiency of ~90% and long-term stability of 50 h.

While such device and process engineering is an attractive approach, the carbonation of CO<sub>2</sub> at a microscopic level, which seems inevitable as long as the local environment is basic, and the subsequent regeneration process across the two components raise concerns about the long-term durability of the cycle. Moreover, the use of alkaline metals raises another issue of metal precipitation.<sup>137,138</sup> Therefore, designing a catalyst to accomplish acidic CO<sub>2</sub>RR without alkaline metals is an imperative subject for tackling both the CO<sub>2</sub> conversion ratio and precipitation problem. One alternative is a metal-heteroatom-involved polymer catalyst, which is compatible with zero-gap CEM cells with deionized water.<sup>131</sup> Such a configuration may contribute to increasing the CO<sub>2</sub> conversion efficiency.

The product selectivity of CO<sub>2</sub>RR is less discussed in most CO<sub>2</sub>RR studies, though the plant process design requires the specification of the product component from the conversion unit to access the cost of the following purification. Krause *et al.*<sup>139</sup> reported the product gas composition in an effort to scale up the CO<sub>2</sub>RR to CO. The ratio of CO<sub>2</sub> in the product gas was 10–50% which significantly depends on the CO<sub>2</sub> flow rate and current density. Since product selectivity is closely linked to operation and structural parameters, it is important to clarify both CO<sub>2</sub> conversion efficiency and product concentration, especially when the CO<sub>2</sub>RR is scaled up.

There have been several recent approaches to engineer selectivity. Rather than a constant potential for electrosynthesis, Timoshenko and colleagues<sup>140</sup> have used electrical pulses to tune the products. This presumably protects the catalyst from poisoning. Liu *et al.*<sup>141</sup> developed pyramidal catalysts, the shape of which presumably controlled the selectivity. While such effects, such as confinement, have long been known, Zhu *et al.*<sup>142</sup> used multilayer pyramids to optimize selectivity by combining geometrical effects with layer sequencing to accelerate the reaction. To reach the requisite selectivity, such synergies in the catalyst (and even electrolyser) design must be exploited.

## 5. Conclusions

For CO<sub>2</sub>RR to be rapidly implemented, it must be scalable and profitable, providing the means and incentive for the procedure. Scalability requires readily available catalysts, electrolytes, and devices that can safely operate with ambient CO<sub>2</sub>. On the other hand, profitability necessitates affordable and durable electrolysers that synthesize value-added products with energy efficient processes at a sufficiently high rate and purity. While nature has had billions of years to perfect photosynthesis, our first intentional use of catalysts for any type of

synthesis can be traced back to just over a century ago, and our efforts on CO<sub>2</sub>RR are even more recent. Nevertheless, our knowledge has grown rapidly. This acceleration can be attributed to continued progress in experimental techniques with the advent of *in operando* measurements to verify the reaction mechanisms, the understanding and development of quantum chemistry to provide the theoretical framework, and now the use of artificial intelligence to examine trends to fill the gaps between experimental results and computational predictions in this multi-dimensional space. Discovery has been advanced by high throughput investigations, yet the promise of CO<sub>2</sub>RR has yet to be realized on an industrial scale especially with perhaps the most important outstanding issues – purity and durability. Given the progress that humanity has made in the exceedingly short time spent investigating viable CO<sub>2</sub>RR, in comparison to the eons nature has had to perfect the process, it is not a question of if we succeed in its realization but when.

## Author contributions

Naohiro Fujinuma: Writing – original draft, writing – review & editing; Samuel Lofland: Conceptualization, writing – review & editing, funding acquisition.

## Conflicts of interest

There are no conflicts to declare.

## Acknowledgements

SEL acknowledges support from Sekisui Chemical Ltd.

## References

- 1 P. S. Adam, G. Borrel and S. Gribaldo, Evolutionary history of carbon monoxide dehydrogenase/acetyl-CoA synthase, one of the oldest enzymatic complexes, *Proc. Natl. Acad. Sci. U. S. A.*, 2018, **115**, E1166–E1173.
- 2 D. C. Harris, Charles David Keeling and the story of atmospheric CO<sub>2</sub> measurements, *Anal. Chem.*, 2010, **82**, 7865–7870.
- 3 J. Giner, Electrochemical reduction of CO<sub>2</sub> on platinum electrodes in acid solutions, *Electrochim. Acta*, 1963, **8**, 857–865.
- 4 T. E. Teeter and P. Van Rysselberghe, Reduction of Carbon Dioxide on Mercury Cathodes, *J. Chem. Phys.*, 1954, **22**, 759–760.
- 5 H. Noda, S. Ikeda, Y. Oda, K. Imai, M. Maeda and K. Ito, Electrochemical Reduction of Carbon Dioxide at Various Metal Electrodes in Aqueous Potassium Hydrogen Carbonate Solution, *Bull. Chem. Soc. Jpn.*, 1990, **63**, 2459–2462.

- 6 N. Furuya and K. Matsui, Electroreduction of carbon dioxide on gas-diffusion electrodes modified by metal phthalocyanines, *J. Electroanal. Chem. Interfacial Electrochem.*, 1989, **271**, 181–191.
- 7 Y. Hori, Electrochemical CO<sub>2</sub> Reduction on Metal Electrodes, *Mod. Aspects Electrochem.*, 2008, 89–189.
- 8 S. Nitopi, E. Bertheussen, S. B. Scott, X. Liu, A. K. Engstfeld, S. Horch, B. Seger, I. E. L. Stephens, K. Chan, *et al.*, Progress and Perspectives of Electrochemical CO<sub>2</sub> Reduction on Copper in Aqueous Electrolyte, *Chem. Rev.*, 2019, **119**, 7610–7672.
- 9 M. Dunwell, W. Luc, Y. Yan, F. Jiao and B. Xu, Understanding Surface-Mediated Electrochemical Reactions: CO<sub>2</sub> Reduction and beyond, *ACS Catal.*, 2018, **8**, 8121–8129.
- 10 S. Vijay, W. Ju, S. Brückner, S. C. Tsang, P. Strasser and K. Chan, Unified mechanistic understanding of CO<sub>2</sub> reduction to CO on transition metal and single atom catalysts, *Nat. Catal.*, 2021, **4**, 1024–1031.
- 11 J. A. Gauthier, M. Fields, M. Bajdich, L. D. Chen, R. B. Sandberg, K. Chan and J. K. Nørskov, Facile Electron Transfer to CO<sub>2</sub> during Adsorption at the Metal|Solution Interface, *J. Phys. Chem. C*, 2019, **123**, 29278–29283.
- 12 Y. Y. Birdja, E. Pérez-Gallent, M. C. Figueiredo, A. J. Göttle, F. Calle-Vallejo and M. T. M. Koper, Advances and challenges in understanding the electrocatalytic conversion of carbon dioxide to fuels, *Nat. Energy*, 2019, **4**, 732–745.
- 13 J. S. Yoo, R. Christensen, T. Vegge, J. K. Nørskov and F. Studt, Theoretical Insight into the Trends that Guide the Electrochemical Reduction of Carbon Dioxide to Formic Acid, *ChemSusChem*, 2016, **9**, 358–363.
- 14 B. Zhang, Y. Chang, Y. Wu, Z. Fan, P. Zhai, C. Wang, J. Gao, L. Sun and J. Hou, Regulating \*OCHO Intermediate as Rate-Determining Step of Defective Oxynitride Nanosheets Enabling Robust CO<sub>2</sub> Electroreduction, *Adv. Energy Mater.*, 2022, **12**, 2200321.
- 15 J. Chen, B. Ma, Z. Xie, W. Li, Y. Yang, M. Mu, X. Zou, B. Zhao and W. Song, Bifunctional porous SnO<sub>2</sub>/Ag nanofibers for efficient electroreduction of carbon dioxide to formate and its mechanism elucidation by *in situ* surface-enhanced Raman scattering, *Appl. Catal., B*, 2023, **325**, 122350.
- 16 S. Verma, S. Lu and P. J. A. Kenis, Co-electrolysis of CO<sub>2</sub> and glycerol as a pathway to carbon chemicals with improved techno-economics due to low electricity consumption, *Nat. Energy*, 2019, **4**, 466–474.
- 17 C. Han, Y. H. Li, J. Y. Li, M. Y. Qi, Z. R. Tang and Y. J. Xu, Cooperative Syngas Production and C–N Bond Formation in One Photoredox Cycle, *Angew. Chem., Int. Ed.*, 2021, **60**, 7962–7970.
- 18 L. Yuan, M. Y. Qi, Z. R. Tang and Y. J. Xu, Coupling Strategy for CO<sub>2</sub> Valorization Integrated with Organic Synthesis by Heterogeneous Photocatalysis, *Angew. Chem., Int. Ed.*, 2021, **60**, 21150–21172.
- 19 SunShot 2030 | Department of Energy, < <https://www.energy.gov/eere/solar/sunshot-2030> > (31 July 2023).
- 20 A. Raksajati, M. T. Ho and D. E. Wiley, Reducing the cost of CO<sub>2</sub> capture from flue gases using aqueous chemical absorption, *Ind. Eng. Chem. Res.*, 2013, **52**, 16887–16901.
- 21 J. B. Greenblatt, D. J. Miller, J. W. Ager, F. A. Houle and I. D. Sharp, The Technical and Energetic Challenges of Separating (Photo)Electrochemical Carbon Dioxide Reduction Products, *Joule*, 2018, **2**, 381–420.
- 22 M. Jouny, W. Luc and F. Jiao, General Techno-Economic Analysis of CO<sub>2</sub> Electrolysis Systems, *Ind. Eng. Chem. Res.*, 2018, **57**, 2165–2177.
- 23 S. Verma, B. Kim, H. R. M. Jhong, S. Ma and P. J. A. Kenis, A Gross-Margin Model for Defining Technoeconomic Benchmarks in the Electroreduction of CO<sub>2</sub>, *ChemSusChem*, 2016, **9**, 1972–1979.
- 24 P. De Luna, C. Hahn, D. Higgins, S. A. Jaffer, T. F. Jaramillo and E. H. Sargent, What would it take for renewably powered electrosynthesis to displace petrochemical processes?, *Science*, 2019, **364**, eaav3506.
- 25 J. M. Spurgeon and B. Kumar, A comparative techno-economic analysis of pathways for commercial electrochemical CO<sub>2</sub> reduction to liquid products, *Energy Environ. Sci.*, 2018, **11**, 1536–1551.
- 26 G. Z. Kyriacou and A. K. Anagnostopoulos, Influence CO<sub>2</sub> partial pressure and the supporting electrolyte cation on the product distribution in CO<sub>2</sub> electroreduction, *J. Appl. Electrochem.*, 1993, **23**, 483–486.
- 27 N. Hidetomo, I. Shoichiro, Y. Akio, E. Hisahiko and I. Kaname, Kinetics of Electrochemical Reduction of Carbon Dioxide on a Gold Electrode in Phosphate Buffer Solutions, *Bull. Chem. Soc. Jpn.*, 2006, **68**, 1889–1895.
- 28 S. Komatsu, M. Tanaka, A. Okumura and A. Kungi, Preparation of Cu-solid polymer electrolyte composite electrodes and application to gas-phase electrochemical reduction of CO<sub>2</sub>, *Electrochim. Acta*, 1995, **40**, 745–753.
- 29 B. Kim, S. Ma, H. R. Molly Jhong and P. J. A. Kenis, Influence of dilute feed and pH on electrochemical reduction of CO<sub>2</sub> to CO on Ag in a continuous flow electrolyzer, *Electrochim. Acta*, 2015, **166**, 271–276.
- 30 Y. Xu, J. P. Edwards, J. Zhong, C. P. O'Brien, C. M. Gabardo, C. McCallum, J. Li, C. T. Dinh, E. H. Sargent, *et al.*, Oxygen-tolerant electroproduction of C<sub>2</sub> products from simulated flue gas, *Energy Environ. Sci.*, 2020, **13**, 554–561.
- 31 T. Arai, S. Sato and T. Morikawa, A monolithic device for CO<sub>2</sub> photoreduction to generate liquid organic substances in a single-compartment reactor, *Energy Environ. Sci.*, 2015, **8**, 1998–2002.
- 32 X. Lu, Z. Jiang, X. Yuan, Y. Wu, R. Malpass-Evans, Y. Zhong, Y. Liang, N. B. McKeown and H. Wang, A bio-inspired O<sub>2</sub>-tolerant catalytic CO<sub>2</sub> reduction electrode, *Sci. Bull.*, 2019, **64**, 1890–1895.
- 33 L. Liao, R. An, H. Li, Y. Xu, J. J. Wu and X. Zhao, Catalytic Access to Functionalized Allylic gem-Difluorides via Fluorinative Meyer–Schuster-Like Rearrangement, *Angew. Chem., Int. Ed.*, 2020, **59**, 11010–11019.

- 34 8.7. Nitrogen Oxides (NO<sub>x</sub>) Emissions | netl.doe.gov, <<https://www.netl.doe.gov/research/Coal/energy-systems/gasification/gasifiedia/nitrogen-oxides>> (31 July 2023).
- 35 B. H. Ko, B. Hasa, H. Shin, E. Jeng, S. Overa, W. Chen and F. Jiao, The impact of nitrogen oxides on electrochemical carbon dioxide reduction, *Nat. Commun.*, 2020, **11**, 1–9.
- 36 B. U. Choi, Y. C. Tan, H. Song, K. B. Lee and J. Oh, System Design Considerations for Enhancing Electroproduction of Formate from Simulated Flue Gas, *ACS Sustainable Chem. Eng.*, 2021, **9**, 2348–2357.
- 37 Y. Zhai, L. Chiachiarrelli and N. Sridhar, Effect of Gaseous Impurities on the Electrochemical Reduction of CO<sub>2</sub> on Copper Electrodes, *ECS Trans.*, 2009, **19**, 1–13.
- 38 D. Kopljar, N. Wagner and E. Klemm, Transferring Electrochemical CO<sub>2</sub> Reduction from Semi-Batch into Continuous Operation Mode Using Gas Diffusion Electrodes, *Chem. Eng. Technol.*, 2016, **39**, 2042–2050.
- 39 H. Yang, J. J. Kaczur, S. D. Sajjad and R. I. Masel, Electrochemical conversion of CO<sub>2</sub> to formic acid utilizing Sustainion™ membranes, *J. CO<sub>2</sub> Util.*, 2017, **20**, 208–217.
- 40 X. Lu, D. Y. C. Leung, H. Wang and J. Xuan, A high performance dual electrolyte microfluidic reactor for the utilization of CO<sub>2</sub>, *Appl. Energy*, 2017, **194**, 549–559.
- 41 S. Ma, M. Sadakiyo, R. Luo, M. Heima, M. Yamauchi and P. J. A. Kenis, One-step electrosynthesis of ethylene and ethanol from CO<sub>2</sub> in an alkaline electrolyzer, *J. Power Sources*, 2016, **301**, 219–228.
- 42 C. Reller, R. Krause, E. Volkova, B. Schmid, S. Neubauer, A. Rucki, M. Schuster and G. Schmid, Selective Electroreduction of CO<sub>2</sub> toward Ethylene on Nano Dendritic Copper Catalysts at High Current Density, *Adv. Energy Mater.*, 2017, **7**, 1602114.
- 43 C. T. Dinh, T. Burdyny, G. Kibria, A. Seifitokaldani, C. M. Gabardo, F. Pelayo García De Arquer, A. Kiani, J. P. Edwards, P. De Luna, *et al.*, CO<sub>2</sub> electroreduction to ethylene via hydroxide-mediated copper catalysis at an abrupt interface, *Science*, 2018, **360**, 783–787.
- 44 Z. Liu, H. Yang, R. Kutz and R. I. Masel, CO<sub>2</sub> Electrolysis to CO and O<sub>2</sub> at High Selectivity, Stability and Efficiency Using Sustainion Membranes, *J. Electrochem. Soc.*, 2018, **165**, J3371–J3377.
- 45 J. J. Kaczur, H. Yang, Z. Liu, S. D. Sajjad and R. I. Masel, Carbon dioxide and water electrolysis using new alkaline stable anion membranes, *Front. Chem.*, 2018, **6**, 377597.
- 46 T. Haas, R. Krause, R. Weber, M. Demler and G. Schmid, Technical photosynthesis involving CO<sub>2</sub> electrolysis and fermentation, *Nat. Catal.*, 2018, **1**, 32–39.
- 47 S. Verma, Y. Hamasaki, C. Kim, W. Huang, S. Lu, H. R. M. Jhong, A. A. Gewirth, T. Fujigaya, N. Nakashima, *et al.*, Insights into the Low Overpotential Electroreduction of CO<sub>2</sub> to CO on a Supported Gold Catalyst in an Alkaline Flow Electrolyzer, *ACS Energy Lett.*, 2018, **3**, 193–198.
- 48 C. M. Gabardo, A. Seifitokaldani, J. P. Edwards, C. T. Dinh, T. Burdyny, M. G. Kibria, C. P. O'Brien, E. H. Sargent and D. Sinton, Combined high alkalinity and pressurization enable efficient CO<sub>2</sub> electroreduction to CO, *Energy Environ. Sci.*, 2018, **11**, 2531–2539.
- 49 K. Jiang, S. Siahrostami, T. Zheng, Y. Hu, S. Hwang, E. Stavitski, Y. Peng, J. Dynes, M. Gangisetty, *et al.*, Isolated Ni single atoms in graphene nanosheets for high-performance CO<sub>2</sub> reduction, *Energy Environ. Sci.*, 2018, **11**, 893–903.
- 50 X. Lu, Y. Wu, X. Yuan, L. Huang, Z. Wu, J. Xuan, Y. Wang and H. Wang, High-Performance Electrochemical CO<sub>2</sub> Reduction Cells Based on Non-noble Metal Catalysts, *ACS Energy Lett.*, 2018, **3**, 2527–2532.
- 51 B. Endrödi, E. Kecsenovity, A. Samu, F. Darvas, R. V. Jones, V. Török, A. Danyi and C. Janáky, Multilayer Electrolyzer Stack Converts Carbon Dioxide to Gas Products at High Pressure with High Efficiency, *ACS Energy Lett.*, 2019, **4**, 1770–1777.
- 52 D. A. Salvatore, D. M. Weekes, J. He, K. E. Dettelbach, Y. C. Li, T. E. Mallouk and C. P. Berlinguette, Electrolysis of Gaseous CO<sub>2</sub> to CO in a Flow Cell with a Bipolar Membrane, *ACS Energy Lett.*, 2018, **3**, 149–154.
- 53 P. Jeanty, C. Scherer, E. Magori, K. Wiesner-Fleischer, O. Hinrichsen and M. Fleischer, Upscaling and continuous operation of electrochemical CO<sub>2</sub> to CO conversion in aqueous solutions on silver gas diffusion electrodes, *J. CO<sub>2</sub> Util.*, 2018, **24**, 454–462.
- 54 P. De Luna, R. Quintero-Bermudez, C. T. Dinh, M. B. Ross, O. S. Bushuyev, P. Todorović, T. Regier, S. O. Kelley, P. Yang, *et al.*, Catalyst electro-redeposition controls morphology and oxidation state for selective carbon dioxide reduction, *Nat. Catal.*, 2018, **1**, 103–110.
- 55 T. T. Zhuang, Z. Q. Liang, A. Seifitokaldani, Y. Li, P. De Luna, T. Burdyny, F. Che, F. Meng, Y. Min, *et al.*, Steering post-C–C coupling selectivity enables high efficiency electroreduction of carbon dioxide to multi-carbon alcohols, *Nat. Catal.*, 2018, **1**, 421–428.
- 56 M. Luo, Z. Wang, Y. C. Li, J. Li, F. Li, Y. Lum, D. H. Nam, B. Chen, J. Wicks, *et al.*, Hydroxide promotes carbon dioxide electroreduction to ethanol on copper via tuning of adsorbed hydrogen, *Nat. Commun.*, 2019, **10**, 1–7.
- 57 F. Li, Y. C. Li, Z. Wang, J. Li, D. H. Nam, Y. Lum, M. Luo, X. Wang, A. Ozden, *et al.*, Cooperative CO<sub>2</sub>-to-ethanol conversion via enriched intermediates at molecule–metal catalyst interfaces, *Nat. Catal.*, 2019, **3**, 75–82.
- 58 F. P. García de Arquer, C. T. Dinh, A. Ozden, J. Wicks, C. McCallum, A. R. Kirmani, D. H. Nam, C. Gabardo, A. Seifitokaldani, *et al.*, CO<sub>2</sub> electrolysis to multicarbon products at activities greater than 1 A cm<sup>-2</sup>, *Science*, 2020, **367**, 661–666.
- 59 X. Wang, Z. Wang, F. P. García de Arquer, C. T. Dinh, A. Ozden, Y. C. Li, D. H. Nam, J. Li, Y. S. Liu, *et al.*, Efficient electrically powered CO<sub>2</sub>-to-ethanol via suppression of deoxygenation, *Nat. Energy*, 2020, **5**, 478–486.
- 60 X. Wang, A. Xu, F. Li, S. F. Hung, D. H. Nam, C. M. Gabardo, Z. Wang, Y. Xu, A. Ozden, *et al.*, Efficient Methane Electrosynthesis Enabled by Tuning Local CO<sub>2</sub> Availability, *J. Am. Chem. Soc.*, 2020, **142**, 3525–3531.

- 61 Z. Yin, H. Peng, X. Wei, H. Zhou, J. Gong, M. Huai, L. Xiao, G. Wang, J. Lu, *et al.*, An alkaline polymer electrolyte CO<sub>2</sub> electrolyzer operated with pure water, *Energy Environ. Sci.*, 2019, **12**, 2455–2462.
- 62 W. Lee, Y. E. Kim, M. H. Youn, S. K. Jeong and K. T. Park, Catholyte-Free Electrocatalytic CO<sub>2</sub> Reduction to Formate, *Angew. Chem., Int. Ed.*, 2018, **57**, 6883–6887.
- 63 J. Lee, J. Lim, C. W. Roh, H. S. Whang and H. Lee, Electrochemical CO<sub>2</sub> reduction using alkaline membrane electrode assembly on various metal electrodes, *J. CO<sub>2</sub> Util.*, 2019, **31**, 244–250.
- 64 R. Xia, S. Zhang, X. Ma and F. Jiao, Surface-functionalized palladium catalysts for electrochemical CO<sub>2</sub> reduction, *J. Mater. Chem. A*, 2020, **8**, 15884–15890.
- 65 Q. Gong, P. Ding, M. Xu, X. Zhu, M. Wang, J. Deng, Q. Ma, N. Han, Y. Zhu, *et al.*, Structural defects on converted bismuth oxide nanotubes enable highly active electrocatalysis of carbon dioxide reduction, *Nat. Commun.*, 2019, **10**, 1–10.
- 66 G. O. Larrazábal, P. Strøm-Hansen, J. P. Heli, K. Zeiter, K. T. Therkildsen, I. Chorkendorff and B. Seger, Analysis of Mass Flows and Membrane Cross-over in CO<sub>2</sub> Reduction at High Current Densities in an MEA-Type Electrolyzer, *ACS Appl. Mater. Interfaces*, 2019, **11**, 41281–41288.
- 67 T. Möller, W. Ju, A. Bagger, X. Wang, F. Luo, T. Ngo Thanh, A. S. Varela, J. Rossmeisl and P. Strasser, Efficient CO<sub>2</sub> to CO electrolysis on solid Ni–N–C catalysts at industrial current densities, *Energy Environ. Sci.*, 2019, **12**, 640–647.
- 68 T. Zheng, K. Jiang, N. Ta, Y. Hu, J. Zeng, J. Liu and H. Wang, Large-Scale and Highly Selective CO<sub>2</sub> Electrocatalytic Reduction on Nickel Single-Atom Catalyst, *Joule*, 2019, **3**, 265–278.
- 69 S. Ren, D. Joulié, D. Salvatore, K. Torbensen, M. Wang, M. Robert and C. P. Berlinguette, Molecular electrocatalysts can mediate fast, selective CO<sub>2</sub> reduction in a flow cell, *Science*, 2019, **365**, 367–369.
- 70 W. H. Cheng, M. H. Richter, I. Sullivan, D. M. Larson, C. Xiang, B. S. Brunshwig and H. A. Atwater, CO<sub>2</sub> Reduction to CO with 19% Efficiency in a Solar-Driven Gas Diffusion Electrode Flow Cell under Outdoor Solar Illumination, *ACS Energy Lett.*, 2020, 470–476.
- 71 J. P. Edwards, Y. Xu, C. M. Gabardo, C. T. Dinh, J. Li, Z. B. Qi, A. Ozden, E. H. Sargent and D. Sinton, Efficient electrocatalytic conversion of carbon dioxide in a low-resistance pressurized alkaline electrolyzer, *Appl. Energy*, 2020, **261**, 114305.
- 72 J. Chen, Z. Wang, H. Lee, J. Mao, C. A. Grimes, C. Liu, M. Zhang, Z. Lu, Y. Chen, *et al.*, Efficient electroreduction of CO<sub>2</sub> to CO by Ag-decorated S-doped g-C<sub>3</sub>N<sub>4</sub>/CNT nanocomposites at industrial scale current density, *Mater. Today Phys.*, 2020, **12**, 100176.
- 73 T. Li, E. W. Lees, M. Goldman, D. A. Salvatore, D. M. Weekes and C. P. Berlinguette, Electrolytic Conversion of Bicarbonate into CO in a Flow Cell, *Joule*, 2019, **3**, 1487–1497.
- 74 Y. C. Li, G. Lee, T. Yuan, Y. Wang, D. H. Nam, Z. Wang, F. P. García De Arquer, Y. Lum, C. T. Dinh, *et al.*, CO<sub>2</sub> Electroreduction from Carbonate Electrolyte, *ACS Energy Lett.*, 2019, **4**, 1427–1431.
- 75 C. Xia, P. Zhu, Q. Jiang, Y. Pan, W. Liang, E. Stavitsk, H. N. Alshareef and H. Wang, Continuous production of pure liquid fuel solutions via electrocatalytic CO<sub>2</sub> reduction using solid-electrolyte devices, *Nat. Energy*, 2019, **4**, 776–785.
- 76 T. Shinagawa, G. O. Larrazábal, A. J. Martín, F. Krumeich and J. Pérez-Ramírez, Sulfur-Modified Copper Catalysts for the Electrochemical Reduction of Carbon Dioxide to Formate, *ACS Catal.*, 2018, **8**, 837–844.
- 77 S. Sen, S. M. Brown, M. L. Leonard and F. R. Brushett, Electroreduction of carbon dioxide to formate at high current densities using tin and tin oxide gas diffusion electrodes, *J. Appl. Electrochem.*, 2019, **49**, 917–928.
- 78 Y. Chen, A. Vise, W. E. Klein, F. C. Cetinbas, D. J. Myers, W. A. Smith, W. A. Smith, W. A. Smith, T. G. Deutsch, *et al.*, A Robust, Scalable Platform for the Electrochemical Conversion of CO<sub>2</sub> to Formate: Identifying Pathways to Higher Energy Efficiencies, *ACS Energy Lett.*, 2020, **5**, 1825–1833.
- 79 J. J. Lv, M. Jouny, W. Luc, W. Zhu, J. J. Zhu and F. Jiao, A Highly Porous Copper Electrocatalyst for Carbon Dioxide Reduction, *Adv. Mater.*, 2018, **30**, 1803111.
- 80 F. Li, A. Thevenon, A. Rosas-Hernández, Z. Wang, Y. Li, C. M. Gabardo, A. Ozden, C. T. Dinh, J. Li, *et al.*, Molecular tuning of CO<sub>2</sub>-to-ethylene conversion, *Nature*, 2020, **577**, 509–513.
- 81 W. Ma, S. Xie, T. Liu, Q. Fan, J. Ye, F. Sun, Z. Jiang, Q. Zhang, J. Cheng, *et al.*, Electrocatalytic reduction of CO<sub>2</sub> to ethylene and ethanol through hydrogen-assisted C–C coupling over fluorine-modified copper, *Nat. Catal.*, 2020, **3**, 478–487.
- 82 M. Zhong, K. Tran, Y. Min, C. Wang, Z. Wang, C. T. Dinh, P. De Luna, Z. Yu, A. S. Rasouli, *et al.*, Accelerated discovery of CO<sub>2</sub> electrocatalysts using active machine learning, *Nature*, 2020, **581**, 178–183.
- 83 C. M. Gabardo, C. P. O'Brien, J. P. Edwards, C. McCallum, Y. Xu, C. T. Dinh, J. Li, E. H. Sargent and D. Sinton, Continuous Carbon Dioxide Electroreduction to Concentrated Multi-carbon Products Using a Membrane Electrode Assembly, *Joule*, 2019, **3**, 2777–2791.
- 84 N. Martić, C. Reller, C. Macauley, M. Löffler, B. Schmid, D. Reinisch, E. Volkova, A. Maltenerberger, A. Rucki, *et al.*, Paramelaconite-Enriched Copper-Based Material as an Efficient and Robust Catalyst for Electrochemical Carbon Dioxide Reduction, *Adv. Energy Mater.*, 2019, **9**, 1901228.
- 85 R. Wang, H. Haspel, A. Pustovarenko, A. Dikhtiarenko, A. Russkikh, G. Shterk, D. Osadchii, S. Ould-Chikh, M. Ma, *et al.*, Maximizing Ag Utilization in High-Rate CO<sub>2</sub> Electrochemical Reduction with a Coordination Polymer-Mediated Gas Diffusion Electrode, *ACS Energy Lett.*, 2019, **4**, 2024–2031.



- 86 S. Ma, R. Luo, J. I. Gold, A. Z. Yu, B. Kim and P. J. A. Kenis, Carbon nanotube containing Ag catalyst layers for efficient and selective reduction of carbon dioxide, *J. Mater. Chem. A*, 2016, **4**, 8573–8578.
- 87 W. Zhu, S. Kattel, F. Jiao and J. G. Chen, Shape-Controlled CO<sub>2</sub> Electrochemical Reduction on Nanosized Pd Hydride Cubes and Octahedra, *Adv. Energy Mater.*, 2019, **9**, 1802840.
- 88 H. R. Molly Jhong, C. E. Tornow, C. Kim, S. Verma, J. L. Oberst, P. S. Anderson, A. A. Gewirth, T. Fujigaya, N. Nakashima, *et al.*, Gold Nanoparticles on Polymer-Wrapped Carbon Nanotubes: An Efficient and Selective Catalyst for the Electroreduction of CO<sub>2</sub>, *ChemPhysChem*, 2017, **18**, 3274–3279.
- 89 L. Ma, W. Hu, Q. Pan, L. Zou, Z. Zou, K. Wen and H. Yang, Polyvinyl alcohol-modified gold nanoparticles with record-high activity for electrochemical reduction of CO<sub>2</sub> to CO, *J. CO<sub>2</sub> Util.*, 2019, **34**, 108–114.
- 90 S. Ma, Y. Lan, G. M. J. Perez, S. Moniri and P. J. A. Kenis, Silver Supported on Titania as an Active Catalyst for Electrochemical Carbon Dioxide Reduction, *ChemSusChem*, 2014, **7**, 866–874.
- 91 Q. Zhu, D. Yang, H. Liu, X. Sun, C. Chen, J. Bi, J. Liu, H. Wu and B. Han, Hollow Metal–Organic-Framework-Mediated In Situ Architecture of Copper Dendrites for Enhanced CO<sub>2</sub> Electroreduction, *Angew. Chem., Int. Ed.*, 2020, **59**, 8896–8901.
- 92 F. Yang, P. L. Deng, Q. Wang, J. Zhu, Y. Yan, L. Zhou, K. Qi, H. Liu, H. S. Park, *et al.*, Metal–organic framework-derived cupric oxide polycrystalline nanowires for selective carbon dioxide electroreduction to C<sub>2</sub> valuables, *J. Mater. Chem. A*, 2020, **8**, 12418–12423.
- 93 K. Yao, Y. Xia, J. Li, N. Wang, J. Han, C. Gao, M. Han, G. Shen, Y. Liu, *et al.*, Metal–organic framework derived copper catalysts for CO<sub>2</sub> to ethylene conversion, *J. Mater. Chem. A*, 2020, **8**, 11117–11123.
- 94 Y. Wang, H. Shen, K. J. T. Livi, D. Raciti, H. Zong, J. Gregg, M. Onadoko, Y. Wan, A. Watson, *et al.*, Copper Nanocubes for CO<sub>2</sub> Reduction in Gas Diffusion Electrodes, *Nano Lett.*, 2019, 8461–8468.
- 95 W. Ju, F. Jiang, H. Ma, Z. Pan, Y. B. Zhao, F. Pagani, D. Rentsch, J. Wang and C. Battaglia, Electrocatalytic Reduction of Gaseous CO<sub>2</sub> to CO on Sn/Cu-Nanofiber-Based Gas Diffusion Electrodes, *Adv. Energy Mater.*, 2019, **9**, 1901514.
- 96 H. Xiang, S. Rasul, B. Hou, J. Portoles, P. Cumpson and E. H. Yu, Copper-Indium Binary Catalyst on a Gas Diffusion Electrode for High-Performance CO<sub>2</sub> Electrochemical Reduction with Record CO Production Efficiency, *ACS Appl. Mater. Interfaces*, 2020, **12**, 601–608.
- 97 K. Ye, Z. Zhou, J. Shao, L. Lin, D. Gao, N. Ta, R. Si, G. Wang and X. Bao, In Situ Reconstruction of a Hierarchical Sn-Cu/SnO<sub>x</sub> Core/Shell Catalyst for High-Performance CO<sub>2</sub> Electroreduction, *Angew. Chem., Int. Ed.*, 2020, **59**, 4814–4821.
- 98 Y. C. Li, Z. Wang, T. Yuan, D. H. Nam, M. Luo, J. Wicks, B. Chen, J. Li, F. Li, *et al.*, Binding Site Diversity Promotes CO<sub>2</sub> Electroreduction to Ethanol, *J. Am. Chem. Soc.*, 2019, **141**, 8584–8591.
- 99 J. C. Lee, J. Y. Kim, W. H. Joo, D. Hong, S. H. Oh, B. Kim, G. Do Lee, M. Kim, J. Oh, *et al.*, Thermodynamically driven self-formation of copper-embedded nitrogen-doped carbon nanofiber catalysts for a cascade electroreduction of carbon dioxide to ethylene, *J. Mater. Chem. A*, 2020, **8**, 11632–11641.
- 100 C. Chen, X. Yan, Y. Wu, S. Liu, X. Zhang, X. Sun, Q. Zhu, H. Wu and B. Han, Boosting the Productivity of Electrochemical CO<sub>2</sub> Reduction to Multi-Carbon Products by Enhancing CO<sub>2</sub> Diffusion through a Porous Organic Cage, *Angew. Chem., Int. Ed.*, 2022, **61**, e202202607.
- 101 C. Chen, X. Yan, S. Liu, Y. Wu, Q. Wan, X. Sun, Q. Zhu, H. Liu, J. Ma, *et al.*, Highly Efficient Electroreduction of CO<sub>2</sub> to C<sub>2</sub>+ Alcohols on Heterogeneous Dual Active Sites, *Angew. Chem., Int. Ed.*, 2020, **59**, 16459–16464.
- 102 C. Yang, H. Shen, A. Guan, J. Liu, T. Li, Y. Ji, A. M. Al-Enizi, L. Zhang, L. Qian, *et al.*, Fast cooling induced grain-boundary-rich copper oxide for electrocatalytic carbon dioxide reduction to ethanol, *J. Colloid Interface Sci.*, 2020, **570**, 375–381.
- 103 W. Luo, J. Zhang, M. Li and A. Züttel, Boosting CO Production in Electrocatalytic CO<sub>2</sub> Reduction on Highly Porous Zn Catalysts, *ACS Catal.*, 2019, **9**, 3783–3791.
- 104 F. Y. Gao, S. J. Hu, X. L. Zhang, Y. R. Zheng, H. J. Wang, Z. Z. Niu, P. P. Yang, R. C. Bao, T. Ma, *et al.*, High-Curvature Transition-Metal Chalcogenide Nanostructures with a Pronounced Proximity Effect Enable Fast and Selective CO<sub>2</sub> Electroreduction, *Angew. Chem., Int. Ed.*, 2020, **59**, 8706–8712.
- 105 A. Löwe, C. Rieg, T. Hierlemann, N. Salas, D. Kopljär, N. Wagner and E. Klemm, Influence of Temperature on the Performance of Gas Diffusion Electrodes in the CO<sub>2</sub> Reduction Reaction, *ChemElectroChem*, 2019, **6**, 4497–4506.
- 106 H. Xiang, H. A. Miller, M. Bellini, H. Christensen, K. Scott, S. Rasul and E. H. Yu, Production of formate by CO<sub>2</sub> electrochemical reduction and its application in energy storage, *Sustainable Energy Fuels*, 2019, **4**, 277–284.
- 107 J. Wang, J. Zou, X. Hu, S. Ning, X. Wang, X. Kang and S. Chen, Heterostructured intermetallic CuSn catalysts: high performance towards the electrochemical reduction of CO<sub>2</sub> to formate, *J. Mater. Chem. A*, 2019, **7**, 27514–27521.
- 108 G. Díaz-Sainz, M. Alvarez-Guerra, J. Solla-Gullón, L. García-Cruz, V. Montiel and A. Irabien, CO<sub>2</sub> electroreduction to formate: Continuous single-pass operation in a filter-press reactor at high current densities using Bi gas diffusion electrodes, *J. CO<sub>2</sub> Util.*, 2019, **34**, 12–19.
- 109 P. Deng, F. Yang, Z. Wang, S. Chen, Y. Zhou, S. Zaman and B. Y. Xia, Metal–Organic Framework-Derived Carbon Nanorods Encapsulating Bismuth Oxides for Rapid and Selective CO<sub>2</sub> Electroreduction to Formate, *Angew. Chem., Int. Ed.*, 2020, **59**, 10807–10813.
- 110 J. Yang, X. Wang, Y. Qu, X. Wang, H. Huo, Q. Fan, J. Wang, L. M. Yang and Y. Wu, Bi-Based Metal–Organic

- Framework Derived Leafy Bismuth Nanosheets for Carbon Dioxide Electroreduction, *Adv. Energy Mater.*, 2020, **10**, 2001709.
- 111 C. Cao, D. D. Ma, J. F. Gu, X. Xie, G. Zeng, X. Li, S. G. Han, Q. L. Zhu, X. T. Wu, *et al.*, Metal–Organic Layers Leading to Atomically Thin Bismuthene for Efficient Carbon Dioxide Electroreduction to Liquid Fuel, *Angew. Chem., Int. Ed.*, 2020, **59**, 15014–15020.
- 112 H. Yang, Y. Wu, Q. Lin, L. Fan, X. Chai, Q. Zhang, J. Liu, C. He and Z. Lin, Composition Tailoring via N and S Codoping and Structure Tuning by Constructing Hierarchical Pores: Metal-Free Catalysts for High-Performance Electrochemical Reduction of CO<sub>2</sub>, *Angew. Chem., Int. Ed.*, 2018, **57**, 15476–15480.
- 113 C. Chen, X. Sun, X. Yan, Y. Wu, H. Liu, Q. Zhu, B. B. A. Bediako and B. Han, Boosting CO<sub>2</sub> Electroreduction on N,P-Co-doped Carbon Aerogels, *Angew. Chem., Int. Ed.*, 2020, **59**, 11123–11129.
- 114 H. Yang, Q. Lin, C. Zhang, X. Yu, Z. Cheng, G. Li, Q. Hu, X. Ren, Q. Zhang, *et al.*, Carbon dioxide electroreduction on single-atom nickel decorated carbon membranes with industry compatible current densities, *Nat. Commun.*, 2020, **11**, 1–8.
- 115 H. Yang, Q. Lin, Y. Wu, G. Li, Q. Hu, X. Chai, X. Ren, Q. Zhang, J. Liu, *et al.*, Highly efficient utilization of single atoms via constructing 3D and free-standing electrodes for CO<sub>2</sub> reduction with ultrahigh current density, *Nano Energy*, 2020, **70**, 104454.
- 116 J. Gu, C. S. Hsu, L. Bai, H. M. Chen and X. Hu, Atomically dispersed Fe<sup>3+</sup> sites catalyze efficient CO<sub>2</sub> electroreduction to CO, *Science*, 2019, **364**, 1091–1094.
- 117 H. Y. Jeong, M. Balamurugan, V. S. K. Choutipalli, E. S. Jeong, V. Subramanian, U. Sim and K. T. Nam, Achieving highly efficient CO<sub>2</sub> to CO electroreduction exceeding 300 mA cm<sup>-2</sup> with single-atom nickel electrocatalysts, *J. Mater. Chem. A*, 2019, **7**, 10651–10661.
- 118 Y. Wang, Z. Jiang, X. Zhang, Z. Niu, Q. Zhou, X. Wang, H. Li, Z. Lin, H. Zheng, *et al.*, Metal Phthalocyanine-Derived Single-Atom Catalysts for Selective CO<sub>2</sub> Electroreduction under High Current Densities, *ACS Appl. Mater. Interfaces*, 2020, **12**, 33795–33802.
- 119 X. Zhang, Y. Wang, M. Gu, M. Wang, Z. Zhang, W. Pan, Z. Jiang, H. Zheng, M. Lucero, *et al.*, Molecular engineering of dispersed nickel phthalocyanines on carbon nanotubes for selective CO<sub>2</sub> reduction, *Nat. Energy*, 2020, **5**, 684–692.
- 120 C. F. Wen, F. Mao, Y. Liu, X. Y. Zhang, H. Q. Fu, L. R. Zheng, P. F. Liu and H. G. Yang, Nitrogen-Stabilized Low-Valent Ni Motifs for Efficient CO<sub>2</sub> Electrocatalysis, *ACS Catal.*, 2020, **10**, 1086–1093.
- 121 M. Wang, K. Torbensen, D. Salvatore, S. Ren, D. Joulié, F. Dumoulin, D. Mendoza, B. Lassalle-Kaiser, U. Işci, *et al.*, CO<sub>2</sub> electrochemical catalytic reduction with a highly active cobalt phthalocyanine, *Nat. Commun.*, 2019, **10**, 1–8.
- 122 K. Chen, M. Cao, Y. Lin, J. Fu, H. Liao, Y. Zhou, H. Li, X. Qiu, J. Hu, *et al.*, Ligand Engineering in Nickel Phthalocyanine to Boost the Electrocatalytic Reduction of CO<sub>2</sub>, *Adv. Funct. Mater.*, 2022, **32**, 2111322.
- 123 K. Torbensen, C. Han, B. Boudy, N. von Wolff, C. Bertail, W. Braun and M. Robert, Iron Porphyrin Allows Fast and Selective Electrocatalytic Conversion of CO<sub>2</sub> to CO in a Flow Cell, *Chem. – Eur. J.*, 2020, **26**, 3034–3038.
- 124 K. Xie, R. K. Miao, A. Ozden, S. Liu, Z. Chen, C. T. Dinh, J. E. Huang, Q. Xu, C. M. Gabardo, *et al.*, Bipolar membrane electrolyzers enable high single-pass CO<sub>2</sub> electroreduction to multicarbon products, *Nat. Commun.*, 2022, **13**, 1–12.
- 125 S. Li, W. Chen, X. Dong, C. Zhu, A. Chen, Y. Song, G. Li, W. Wei and Y. Sun, Hierarchical micro/nanostructured silver hollow fiber boosts electroreduction of carbon dioxide, *Nat. Commun.*, 2022, **13**, 1–9.
- 126 Y. Wang, Z. Wang, C. T. Dinh, J. Li, A. Ozden, M. Golam Kibria, A. Seifitokaldani, C. S. Tan, C. M. Gabardo, *et al.*, Catalyst synthesis under CO<sub>2</sub> electroreduction favours faceting and promotes renewable fuels electrosynthesis, *Nat. Catal.*, 2019, **3**, 98–106.
- 127 T. Zhang, J. C. Bui, Z. Li, A. T. Bell, A. Z. Weber and J. Wu, Highly selective and productive reduction of carbon dioxide to multicarbon products via in situ CO management using segmented tandem electrodes, *Nat. Catal.*, 2022, **5**, 202–211.
- 128 J. H. Guo, X. Y. Zhang, X. Y. Dao and W. Y. Sun, Nanoporous Metal–Organic Framework-Based Ellipsoidal Nanoparticles for the Catalytic Electroreduction of CO<sub>2</sub>, *ACS Appl. Nano Mater.*, 2020, **3**, 2625–2635.
- 129 J. R. Huang, X. F. Qiu, Z. H. Zhao, H. L. Zhu, Y. C. Liu, W. Shi, P. Q. Liao and X. M. Chen, Single-Product Faradaic Efficiency for Electrocatalytic of CO<sub>2</sub> to CO at Current Density Larger than 1.2 A cm<sup>-2</sup> in Neutral Aqueous Solution by a Single-Atom Nanozyme, *Angew. Chem., Int. Ed.*, 2022, **61**, e202210985.
- 130 B. Endrđi, E. Kecsenovity, A. Samu, T. Halmágyi, S. Rojas-Carbonell, L. Wang, Y. Yan and C. Janáky, High carbonate ion conductance of a robust PiperION membrane allows industrial current density and conversion in a zero-gap carbon dioxide electrolyzer cell, *Energy Environ. Sci.*, 2020, **13**, 4098–4105.
- 131 N. Fujinuma, A. Ikoma and S. E. Lofland, Highly Efficient Electrochemical CO<sub>2</sub> Reduction Reaction to CO with One-Pot Synthesized Co-Pyridine-Derived Catalyst Incorporated in a Nafion-Based Membrane Electrode Assembly, *Adv. Energy Mater.*, 2020, **10**, 2001645.
- 132 J. A. Rabinowitz and M. W. Kanan, The future of low-temperature carbon dioxide electrolysis depends on solving one basic problem, *Nat. Commun.*, 2020, **11**, 1–3.
- 133 M. Ma, E. L. Clark, K. T. Therkildsen, S. Dalsgaard, I. Chorkendorff and B. Seger, Insights into the carbon balance for CO<sub>2</sub> electroreduction on Cu using gas diffusion electrode reactor designs, *Energy Environ. Sci.*, 2020, **13**, 977–985.
- 134 E. R. Cofell, U. O. Nwabara, S. S. Bhargava, D. E. Henckel and P. J. A. Kenis, Investigation of Electrolyte-Dependent Carbonate Formation on Gas Diffusion Electrodes for CO<sub>2</sub>

- Electrolysis, *ACS Appl. Mater. Interfaces*, 2021, **13**, 15132–15142.
- 135 C. P. O'Brien, R. K. Miao, S. Liu, Y. Xu, G. Lee, A. Robb, J. E. Huang, K. Xie, K. Bertens, *et al.*, Single Pass CO<sub>2</sub> Conversion Exceeding 85% in the Electrosynthesis of Multicarbon Products via Local CO<sub>2</sub> Regeneration, *ACS Energy Lett.*, 2021, **6**, 2952–2959.
- 136 B. Pan, J. Fan, J. Zhang, Y. Luo, C. Shen, C. Wang, Y. Wang and Y. Li, Close to 90% Single-Pass Conversion Efficiency for CO<sub>2</sub> Electroreduction in an Acid-Fed Membrane Electrode Assembly, *ACS Energy Lett.*, 2022, **7**, 4224–4231.
- 137 J. Disch, L. Bohn, S. Koch, M. Schulz, Y. Han, A. Tengattini, L. Helfen, M. Breitwieser and S. Vierrath, High-resolution neutron imaging of salt precipitation and water transport in zero-gap CO<sub>2</sub> electrolysis, *Nat. Commun.*, 2022, **13**, 1–9.
- 138 S. Garg, Q. Xu, A. B. Moss, M. Mirolo, W. Deng, I. Chorkendorff, J. Drnec and B. Seger, How alkali cations affect salt precipitation and CO<sub>2</sub> electrolysis performance in membrane electrode assembly electrolyzers, *Energy Environ. Sci.*, 2023, **16**, 1631–1643.
- 139 R. Krause, D. Reinisch, C. Reller, H. Eckert, D. Hartmann, D. Taroata, K. Wiesner-Fleischer, A. Bulan, A. Lueken, *et al.*, Industrial Application Aspects of the Electrochemical Reduction of CO<sub>2</sub> to CO in Aqueous Electrolyte, *Chem. Ing. Tech.*, 2020, **92**, 53–61.
- 140 J. Timoshenko, A. Bergmann, C. Rettenmaier, A. Herzog, R. M. Arán-Ais, H. S. Jeon, F. T. Haase, U. Hejral, P. Grosse, *et al.*, Steering the structure and selectivity of CO<sub>2</sub> electroreduction catalysts by potential pulses, *Nat. Catal.*, 2022, **5**, 259–267.
- 141 S. Liu, H. Tao, L. Zeng, Q. Liu, Z. Xu, Q. Liu and J. L. Luo, Shape-Dependent Electrocatalytic Reduction of CO<sub>2</sub> to CO on Triangular Silver Nanoplates, *J. Am. Chem. Soc.*, 2017, **139**, 2160–2163.
- 142 Y. Zhu, Z. Gao, Z. Zhang, T. Lin, Q. Zhang, H. Liu, L. Gu and W. Hu, Selectivity regulation of CO<sub>2</sub> electroreduction on asymmetric AuAgCu tandem heterostructures, *Nano Res.*, 2022, **15**, 7861–7867.